Restoring Occluded Regions Using FW-PCA for Face Recognition

Tomoki Hosoi, Sei Nagashima, Koji Kobayashi
Azbil Corporation,
1–12–2 Kawana, Fujisawa,
251–8522 Japan.
t.hosoi.sh@azbil.com

Koichi Ito, Takafumi Aoki
Graduate School of Information Sciences,
Tohoku University,
6–6–05, Aramazki Aza Aoba, Sendai,
980–8579 Japan.
ito@aoki.ecei.tohoku.ac.jp

Abstract

Occlusions in face images such as eyeglasses, hairs and whiskers decrease the performance of face recognition algorithms. Addressing this problem, this paper proposes a method for restoring occluded regions in face images. The proposed method employs Fast Weighted Principal Component Analysis (FW-PCA), which computes PCA only with effective pixels. The use of FW-PCA makes it possible to detect and restore occluded regions in face images. Through a set of experiments using public face databases, we demonstrate the effectiveness of the proposed method compared with the conventional methods.

1. Introduction

Occlusions in face images such as eyeglasses, hairs, etc. are a major cause to decrease the performance of face recognition algorithms. To improve the performance of the face recognition algorithms, it is required to detect and restore occluded regions in the face image. So far, the occluded-region restoration methods have been reported in Refs. [15, 13, 14, 8, 9]. These methods can be broadly classified into model-based and appearance-based methods.

The model-based methods [15, 13, 14] extract facial feature points by fitting the face models [2, 3, 1] such as Active Appearance Model (AAM) to the face image, and detect occluded regions according to the position of feature points on the face image. Although the accurate occluded regions can be detected if the model fitting is successfully applied, the model fitting approach is not robust against the occluded regions in the face image. On the other hand, the appearance-based methods [8, 9] detect and restore occluded regions using texture information of the face images. Although the detection accuracy of occluded regions for the appearance-based methods may be lower than that for the model-based methods, the appearance-based methods are successfully applied if the occluded regions is not too large compared with the face region. Also, the appearance-based methods can be applied to generic objects. In this paper, we focus on the appearance-based methods to detect and restore occluded regions in the face image.

In the appearance-based methods, Principal Component Analysis (PCA) is the fundamental technique for image reconstruction. Image reconstruction using PCA computes the principal component scores from a part of the input image and reconstructs the whole input image according to the principal component scores. Using only effective pixels which are not occlusion, occluded regions can be reconstructed by using PCA. The reconstruction accuracy depends on the detection accuracy of occluded regions, since it is necessary to accurately detect occluded regions and compute the principal component scores only from the effective pixels.

Refs. [7, 12] have proposed the method to compute the principal component scores from images with occluded regions using multiple sampling sets. Leonardis *et al.* [7] have reconstructed occluded regions of the input image by weighted PCA using a set of pixels randomly selected from the input image. This method may take several minutes, since it is required to compute weighted PCA using least squares optimization. Storer *et al.* [12] have proposed Fast Robust PCA (FR-PCA) which detects the effective pixels using small eigenspaces computed from pixels randomly selected from training images and reconstructs the input image using the detected effective pixels. FR-PCA is required to store all the small subspaces computed in the training process and cannot detect the whole occluded regions.

Addressing the above problems, this paper proposes Fast Weighted PCA (FW-PCA) and the novel occluded-region restoration method using FW-PCA for face recognition. Unlike FR-PCA, the proposed FW-PCA can compute the

978-1-4673-1612-5/12/$31.00 ©2012 IEEE

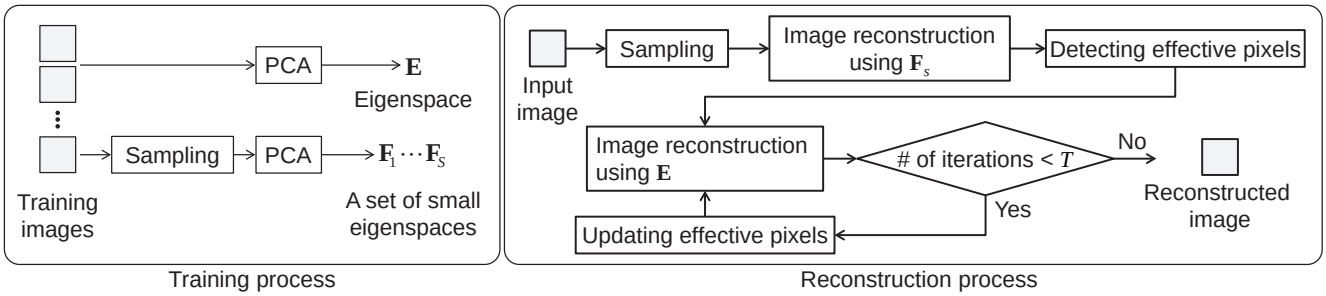

Figure 1. Flow diagram of image reconstruction using FR-PCA.

principal component scores from a part of pixels of the input image using only the eigenspace of training images. The proposed restoration method can detect the reliable position of the occluded regions by iteratively updating the weight of FW-PCA and restore the occluded regions according to the position of the detected occluded regions. Through a set of experiments using public face databases such as FRGC [5], MBGC [10], FERET [11] and Multi-PIE [6], we demonstrate the effectiveness of the proposed method compared with the conventional methods.

2. Related Work

In this section, we briefly introduce the image reconstruction methods using PCA [7] and FR-PCA [12].

2.1. Image Reconstruction Using PCA

Let $\mathbf{x}_l = [x_{l1}\ x_{l2}\ \cdots\ x_{lN}]^{\mathrm{T}}$ be an N-dimensional vector consisting of pixel values $(x_{l1}, x_{l2}, \cdots, x_{lN})$ of the training image. Let $\mathbf{X} = [\mathbf{x}_1\ \mathbf{x}_2\ \cdots\ \mathbf{x}_L]$ be the training images, where L is the number of images. We calculate the covariance matrix from $\mathbf{X}$ and obtain the eigenspace $\mathbf{E}$ which consists of eigenvectors $[\mathbf{e}_1\ \mathbf{e}_2\ \cdots\ \mathbf{e}_D]$ $(D \leq L)$. Using the eigenspace $\mathbf{E}$ calculated by PCA, the reconstructed image $\hat{\mathbf{x}}$ is obtained by

$$\hat{\mathbf{x}} \simeq \mathbf{E}\mathbf{p} \quad \left(\Leftarrow \hat{x}_i \simeq \sum_{d=1}^{D} e_{di} p_d \right), \tag{1}$$

where $\mathbf{p}$ indicates the principal component scores and is calculated by projecting the input image $\mathbf{x}$ onto the eigenspace $\mathbf{E}$ as

$$\mathbf{p} = \mathbf{E}^{\mathrm{T}}\mathbf{x} \quad \left(\Leftarrow p_d = \sum_{i=1}^{N} e_{di} x_i \right). \tag{2}$$

In the case that the missing pixels such as occlusion are included in the input image, the reliability of the principal component score $\mathbf{p}$ is not high. Addressing this problem, the principal component score $\mathbf{p}$ is calculated only from a set of the effective pixels $\mathbf{H}$ in the input image. The reconstruction error $C(\mathbf{p})$ in a set of effective pixels is defined by

$$C(\mathbf{p}) = \sum_{i \in \mathbf{H}} (x_i - \hat{x}_i)^2 = \sum_{i \in \mathbf{H}} \left(x_i - \sum_{d=1}^{D} e_{di} p_d \right)^2. \tag{3}$$

The principal component score $\hat{\mathbf{p}}$ having minimum reconstruction error $C(\mathbf{p})$ is estimated by using the least squares optimization. If the missing pixels of the input image are correctly selected, we can reconstruct the input image using weighted PCA as described above. On the other hand, image reconstruction using weighted PCA with the least squares optimization takes more time than the general PCA.

2.2. Image Reconstruction Using FR-PCA

We describe the image reconstruction method using FR-PCA. This method detects the effective pixels of the input image using small eigenspaces generated from randomly sampled pixels of the training images and reconstructs the input image. Fig. 1 shows a flow diagram of the image reconstruction method using FR-PCA which consists of (i) training process and (ii) reconstruction process.

(i) Training process

First, the eigenspace $\mathbf{E}$ is computed using all the training images. Next, M pixels are extracted from each training image according to S random sampling patterns. Then, the small eigenspace $\mathbf{F}_s$ $(s = 1, \cdots, S)$ is computed for each sampling pattern.

(ii) Reconstruction process

Subsamplings $\mathbf{y}_s$ $(s = 1, \cdots, S)$ are generated from the input image according to S random sampling patterns used in the training process. For each $\mathbf{y}_s$, the reconstructed image $\hat{\mathbf{y}}_s$ is estimated by using the corresponding small eigenspace $\mathbf{F}_s$. Then, the reconstruction error $\mathbf{r}_s$ is obtained by

$$\mathbf{r}_s = |\mathbf{y}_s - \hat{\mathbf{y}}_s|. \tag{4}$$

According to the reconstruction error $\mathbf{r}_s$, the effective pixels are detected. j-th pixel of the subsampling $\mathbf{y}_s$ is removed as a missing pixel, if the reconstruction error r_{sj} satisfies the following condition

$$r_{sj} > \mu_s \bar{r}_s \quad \text{or} \quad r_{sj} > \bar{r}, \tag{5}$$

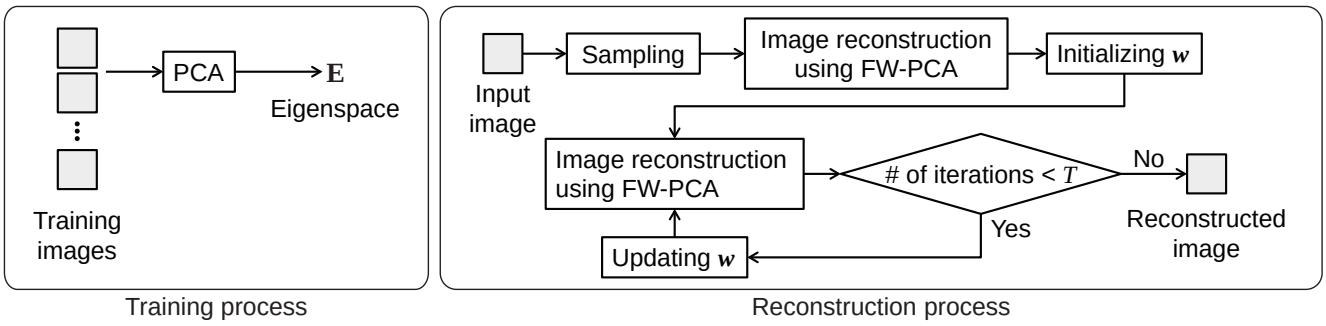

Figure 2. Flow diagram of image reconstruction using FW-PCA.

where $\bar{r}_s$ is the average of the reconstruction error $\mathbf{y}_s$, $\bar{r}$ is the average of all the reconstruction errors, μ_s is a parameter value depending on $\bar{r}_s$. Among the remaining pixels, i.e., the effective-pixel candidates, K pixels are selected in ascending order of the reconstruction error $\mathbf{r_s}$ as a set of effective pixels $\mathbf{H}$.

The input image is reconstructed by using Eq. (3) and the estimated effective pixels $\mathbf{H}$. However, the missing pixels may be included in $\mathbf{H}$. To reduce the missing pixels in $\mathbf{H}$, the pixels having a large error between the input and reconstructed images are removed from $\mathbf{H}$. After T-time iterations of the above process, we obtain the reconstructed image. Note that the above iteration process is repeated until the effective pixels are reduced to the specified number in Ref. [12]. In this paper, we employ the number of iterations to compare the conventional method using FR-PCA with the proposed method.

As described above, the use of FR-PCA makes it possible to achieve fast and robust image reconstruction. On the other hand, this method is required to hold the small eigenspaces $\mathbf{F}_s$ and to iteratively perform weighted PCA with the least squares optimization. Also, this method cannot detect the whole occluded regions in the input image.

3. Image reconstruction using FW-PCA

This section describes FW-PCA and the image reconstruction method using FW-PCA proposed in this paper.

3.1. FW-PCA

The key idea of FW-PCA is to reduce the computation time of the principal component scores by approximating the correlation coefficient between the input image and the eigenvectors and the amplitude of the input image.

The d-th principal component score p_d can be calculated by the inner product of the input image $\mathbf{x}$ and the d-th eigenvector $\mathbf{e}_d$ as follows

$$p_d = \sum_{i=1}^{N} e_{di} x_i = \|\mathbf{e}_d\| \|\mathbf{x}\| \cos\theta_d, \tag{6}$$

where $\|\mathbf{x}\|$ and $\|\mathbf{e}_d\|$ indicate the amplitude of the input image and the d-th eigenvector, respectively. $\cos\theta_d$ indicates the correlation coefficient between the input image and the d-th eigenvector. If the input image has the missing pixels, $\cos\theta_d$ and $\|\mathbf{x}\|$ cannot be directly calculated. Therefore, $\cos\hat{\theta}_d$ and $\|\hat{\mathbf{x}}\|$ are approximated by

$$\cos\hat{\theta}_d = \frac{\sum_{i=1}^{N} w_i e_{di} x_i}{\sqrt{\sum_{i=1}^{N} w_i x_i^2}\sqrt{\sum_{i=1}^{N} w_i e_{di}^2}}, \tag{7}$$

$$\|\hat{\mathbf{x}}\| = \frac{\sqrt{\sum_{i=1}^{N} e_{di}^2}\sqrt{\sum_{i=1}^{N} w_i x_i^2}}{\sqrt{\sum_{i=1}^{N} w_i e_{di}^2}}, \tag{8}$$

where $\mathbf{w} = [w_1\ w_2\ \cdots w_N]^{\mathrm{T}}$ is a weight and each element w_i is assigned 1 for the effective pixel or 0 for the missing pixel. Replacing $\cos\theta_d$ and $\|\mathbf{x}\|$ with Eq. (7) and Eq. (8), respectively, Eq. (6) can be rewritten as

$$\hat{p}_d = \|\mathbf{e}_d\| \|\hat{\mathbf{x}}\| \cos\hat{\theta}_d = \frac{\sum_{i=1}^{N} e_{di}^2 \sum_{i=1}^{N} w_i e_{di} x_i}{\sum_{i=1}^{N} w_i e_{di}^2}. \tag{9}$$

Note that Eq. (9) is equivalent to Eq. (6) if the input image has no missing pixel.

As descrived above, the use of FW-PCA makes it possible to quickly calculate the weighted PCA for the input image having the missing pixels, while the conventional PCA-based method needs to iteratively calculate the principal component scores using the least squares optimization.

3.2. Image Reconstruction Using FW-PCA

We describe the image reconstruction method using FW-PCA. Fig. 2 shows a flow diagram of the image reconstruction method using FW-PCA which consists of (i) training process and (ii) reconstruction process.

(i) Training process

The eigenspace $\mathbf{E}$ is computed using all the training images. The standard deviation of the reconstruction error for each pixel $\sigma = [\sigma_1\ \sigma_2\ \cdots \sigma_N]^{\mathrm{T}}$ is also computed.

(ii) Reconstruction process

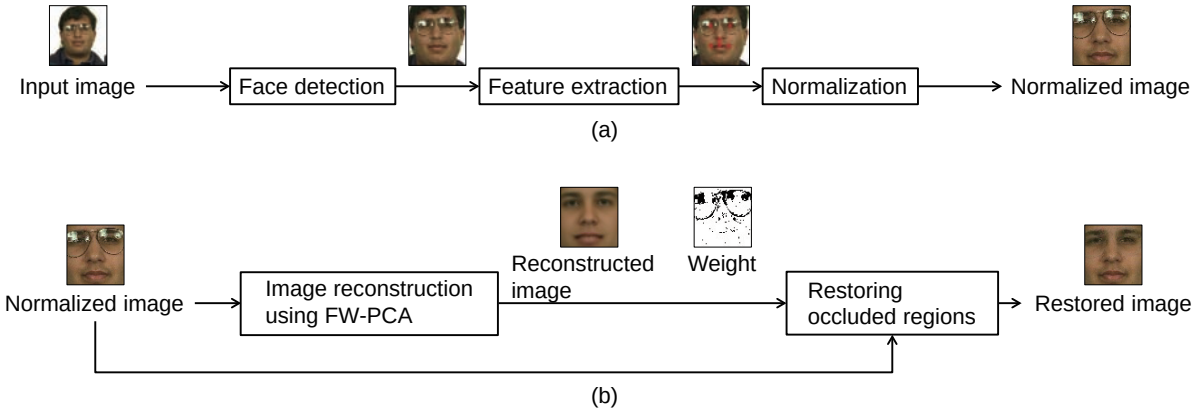

Figure 3. Flow diagram of the proposed method: (a) preprocessing and (b) occluded-region restoration.

First, the initial weight for FW-PCA is determined using the subsamplings of the input image. M pixels are extracted from the input image according to S random sampling patterns. Considering the extracted pixels as the effective pixels, the reconstructed image $\hat{\mathbf{x}}_s$ $(s = 1, \cdots, S)$ for each sampling pattern is computed by using FW-PCA, i.e., Eq. (9). Then, the reconstruction error $\mathbf{r}_s$ between $\mathbf{x}$ and $\hat{\mathbf{x}}_s$ is obtained by

$$\mathbf{r}_s = |\mathbf{x} - \hat{\mathbf{x}}_s|. \tag{10}$$

According to Eq. (5), the initial value of the weight is determined.

The reconstructed image $\hat{\mathbf{x}}$ is obtained by FW-PCA with the input image $\mathbf{x}$ and the weight $\mathbf{w}$. Comparing the reconstructed image $\hat{\mathbf{x}}$ and the input image $\mathbf{x}$, the weight $\mathbf{w}$ is updated by

$$w_i = \begin{cases} 1 & \text{if } (|\hat{x}_i - x_i| < \theta_i) \\ 0 & \text{otherwise} \end{cases} \quad (i = 1, \cdots, N), \tag{11}$$

where $\theta_i = \eta\sigma_i$ is the threshold for each pixel and η is a coefficient for σ_i. After T-time iterations of the above process, we obtain the reconstructed image $\hat{\mathbf{x}}$ and the weight $\mathbf{w}$ which represents occluded regions in the input image. In addition, the above method can be applied to the color images by using the same weight $\mathbf{w}$ for each color channel.

4. Occluded-Region Restoration Using FW-PCA for Face Recognition

We apply the image reconstruction method using FW-PCA to the occluded-region restoration method for face recognition. The proposed method consists of the training process and the restoration process.

4.1. Training process

The training images are normalized by (i) face detection, (ii) feature point extraction and (iii) geometric normalization as shown in Fig. 3 (a). In the step (i), for each training image, the face region is extracted using face detector [16]. In the step (ii), 6 feature points on eyes, nose and mouth are extracted using facial feature point detector [4]. In the final step (iii), for each training image, parameters of linear transformation are estimated by using Procrustes analysis based on the feature points on the average face image $\bar{\mathbf{x}}$ generated from all the training images, and then the position of the training image is normalized. The pixel values of training images are also normalized so that they has a prespecified mean and variance. After normalization, the eigenspace $\mathbf{E}$ and the standard deviation of the reconstruction error σ are computed from the normalized training images.

4.2. Restoration process

The restoration process consists of (i) preprocessing, (ii) image reconstruction using FW-PCA and (iii) occluded-region restoration as shown in Figs. 3 (a) and (b).

(i) Preprocessing

The input image is normalized as well as the training images. The face region of the input image is extracted by using the face detector [16]. The facial feature points are detected by using the facial feature point detector [4]. The position of the input image is normalized by using Procrustes analysis so as to minimize the distance between the feature points on the average face image $\bar{\mathbf{x}}$ and the input image. Thus, we have the normalized input image $\mathbf{x}$.

(ii) Image reconstruction using FW-PCA

The normalized input image $\mathbf{x}$ is reconstructed using the method described in Sect. 3.2. Note that the pixel values of $\mathbf{x}$ is normalized so that they have the same mean and variance of $\bar{\mathbf{x}}$ during each iteration. The pixel values of effective pixels in the final reconstructed image $\hat{\mathbf{x}}$ is normalized so that they have the same mean and variance of the normalized input image $\mathbf{x}$.

(iii) Occluded-region restoration

As mentioned above, we reconstruct the whole input image using the eigenspace $\mathbf{E}$. The reconstructed image $\hat{\mathbf{x}}$

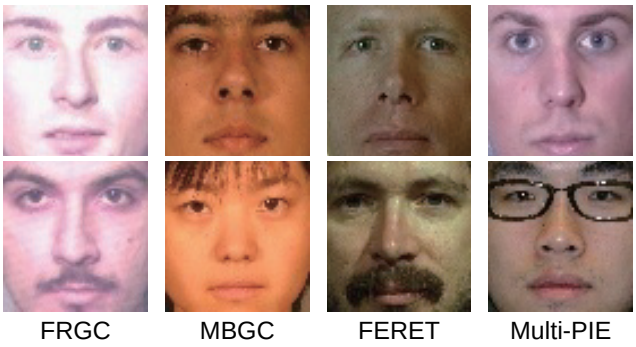

Figure 4. Examples of face images used in the experiments (upper: face image without occlusions, and lower: face image with occlusions).

may result in the smoothed image of the input image $\mathbf{x}$. Therefore, only the missing pixels of the input image $\mathbf{x}$ are replaced by the pixels of the reconstructed image $\hat{\mathbf{x}}$. The restored image $\tilde{\mathbf{x}}$ is obtained by

$$\tilde{x}_i = \begin{cases} x_i & \text{if } w_i = 1 \\ \hat{x}_i & \text{otherwise} \end{cases} \quad (i = 1, \cdots, N). \tag{12}$$

Finally, we can restore only the occluded regions of the input image.

5. Experiments and Discussion

This section describes the performance evaluation of the proposed method using the public face databases. In order to exhibit the effectiveness of the proposed method, we compare the proposed algorithm with the PCA-based method described in Sect. 2.1 and the FR-PCA-based method described in Sect. 2.2.

5.1. Experimental Condition

In the experiments, we use the public face databases such as FRGC [5], MBGC [10], FERET [11] and Multi-PIE [6]. From these databases, we select 5,000 frontal face images as the sample images, where 4,500 images have no occlusions such as eyeglasses, hairs and whiskers and the remaining 500 images have some kind of occlusions on the faces. From 4,500 images without occlusions, 4,000 images are used as the training images and the remaining 500 images are used as the input images. All the 500 images with occlusions are used as the input images.

Fig. 4 shows examples of face images used in the experiments. These face images are 64×64-pixel normalized images obtained by preprocessing. The experiments are performed using both gray-scale and color images.

Table 1 shows a set of parameters for each method. The performance of FR-PCA is evaluated by changing the number of effective pixels K, while the performance of the proposed method is evaluated by changing the number of iterations T. The other parameters are determined so that the computation time of FR-PCA is comparable with that of the proposed method.

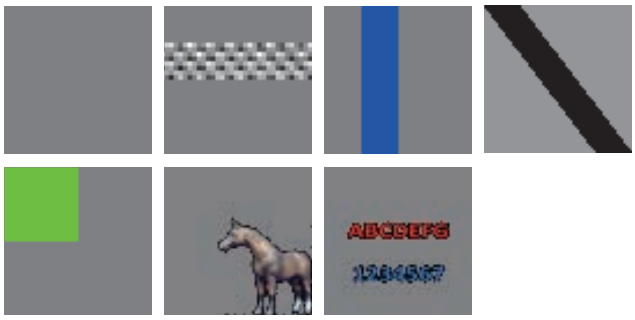

Figure 5. Occluded patterns used in the experiments (gray region indicates the effective pixels).

Table 1. A set of parameters for each method.

	PCA	FR-PCA	Proposed
# of dimensions D	32		
# of sampling patterns S	—	1024	
# of sampling points M	—	256	
# of effective pixels K	—	256, 512, 1024, 2048	2048
# of iterations T	—	4	0, 1, 2, 4
Coefficient η	—		2

In order to evaluate the reconstruction accuracy, each input image is added to the seven occlusion patterns as shown in Fig. 5. The input images with occlusion patterns are restored using the procedure described in Sect. 4. In the case of PCA and FR-PCA, PCA and FR-PCA based image reconstruction methods are used instead of FW-PCA in the step (ii) of the restoration process. In the step (iii) of the restoration process, the final weight $\mathbf{w}$ obtained by each method is used to restore the occluded regions. Note that the reconstructed and restored images obtained by PCA are the same, since the weight $\mathbf{w}$ is always 1.

5.2. Experimental Results and Discussion

Fig. 6 shows an example of the experimental results. The upper, middle and lower rows are the reconstructed image, the weight and the restored image, respectively. The white and black pixels of the weight indicate the effective and missing pixels, respectively. FR-PCA can recover the occluded region, while the reconstruction accuracy is not so high, since the number of the effective pixels for computing the weighted PCA is not enough to reconstruct the images. The proposed method can completely recover the occluded region, since the occluded region is correctly detected from

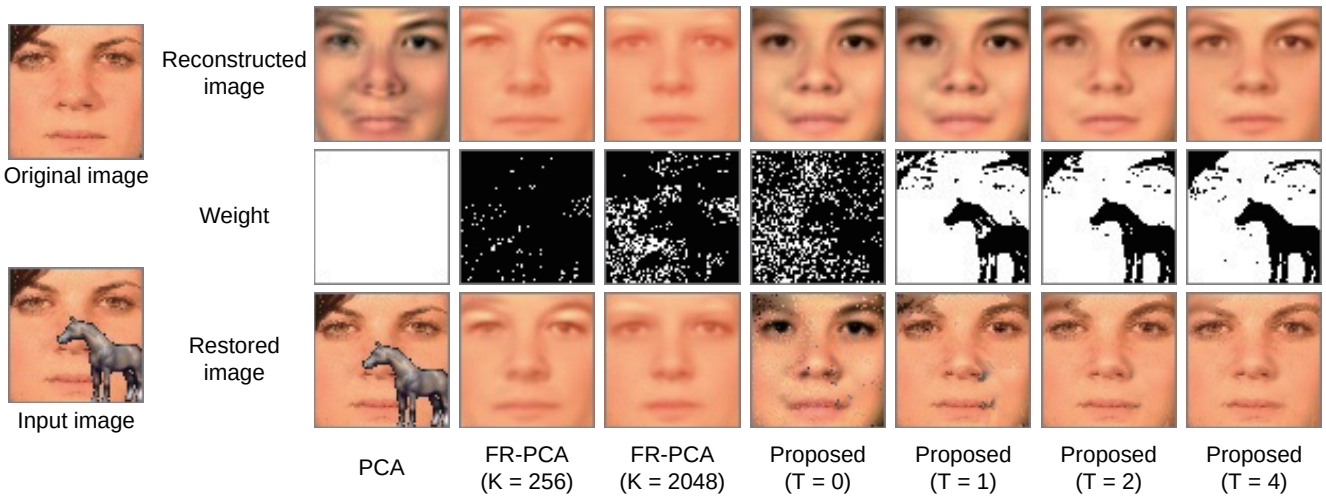

Figure 6. Experimental results of occluded region reconstruction using the conventional methods and the proposed method (upper: reconstructed image, middle: occluded region (weight w) and lower: restored image).

the weight. We empirically confirm that the reconstruction results of the proposed method is converged within $T = 4$. Figs. 7 and 8 show the restored results of each method for gray-scale and color images, respectively. The use of the proposed method makes it possible to recover the occluded regions correctly both gray-scale and color images compared with the conventional methods.

We show the quantitative evaluation results for the conventional and proposed methods. In order to perform the quantitative performance evaluation, we use 500 images without occlusion. The 500 images are added to the seven occlusion patterns as shown in Fig. 5 and are restored by using the conventional and proposed methods. The restoration accuracy is evaluated by the Root Mean Square (RMS) error between the original and the reconstructed or restored images. In addition, the computation time is evaluated on Intel Core2 Duo (2.2GHz) with C++ implementation of the methods.

Tables 2 and 3 show the experimental results for gray-scale and color images, respectively. In the case of the input image without occlusions, the RMS errors of the reconstructed images for FR-PCA and the proposed method are high, since the input images are reconstructed by projecting the effective pixels onto the eigenspace. The RMS errors of the restored images for the proposed method become lower than those of the reconstructed images, since the proposed method can correctly detect the occlusions from the weight. On the other hand, in the restoration process, FR-PCA selects the pixel values of the reconstructed image for most of pixels, since FR-PCA detects the occlusions only on the sampling points. Hence, the RMS errors of the restored images for FR-PCA is comparable with those of the reconstructed images. In the case of the input image with occlusions, the RMS errors become higher than those without occlusions. Among the experimental results, the RMS errors for the proposed method become lower by increasing the number of iterations T. As for $T = 2, 4$, the RMS errors of the restored images is about 5 pixel values. This fact means that the restored images are almost the same as the

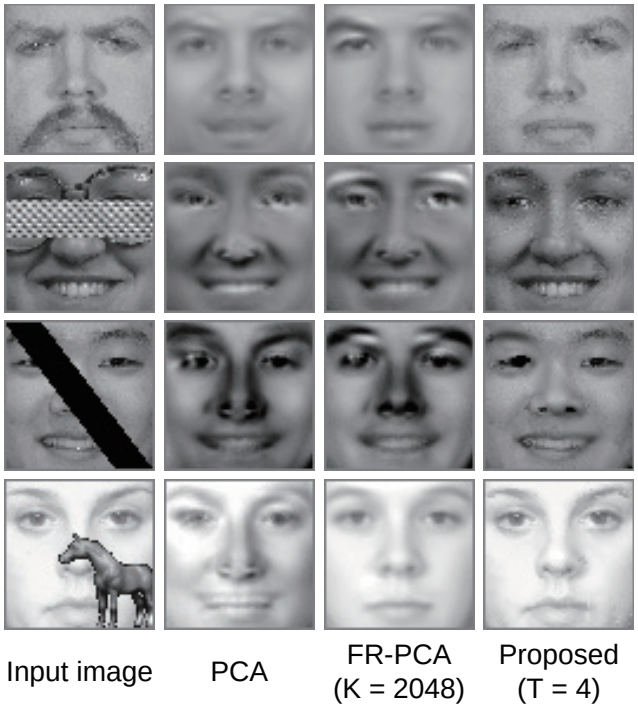

Figure 7. Experimental results for gray-scale images (the results of PCA are the reconstructed images and the results of FR-PCA and the proposed method are the restored images).

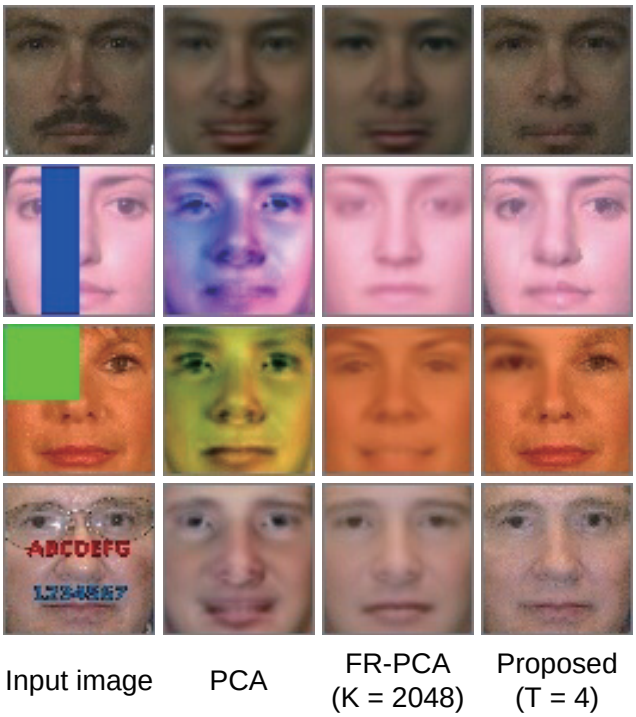

Figure 8. Experimental results for color images (the results of PCA are the reconstructed images and the results of FR-PCA and the proposed method are the restored images).

original images.

The average computation time of the proposed method is about 60 msec and 150msec for the gray-scale and color images, respectively. In terms of the computation time, FR-PCA with $K = 256$ is faster than the proposed method, while the RMS error of FR-PCA with $K = 256$ is highest. Although the computation time of the proposed method is between FR-PCA with $K = 1024$ and $K = 2048$, the RMS errors for the proposed method are lower than those for FR-PCA. Comparing the number of iterations for the proposed method, the proposed method with $T = 2$ is the most balanced one in terms of the computation time and the restoration accuracy.

As is observed the above experimental results, the use of the proposed method makes it possible to achieve fast and accurate occlusion restoration for face images compared with the conventional methods.

6. Conclusion

This paper has proposed a method for detecting and restoring occluded regions for face recognition. The proposed method employs FW-PCA, which computes PCA only with the effective pixels. Through a set of experiments using public face databases, we have demonstrated the effectiveness of the proposed method compared with the conventional methods. The use of the proposed method makes it possible to register face images without occlusions on the face recognition system and to result in improving the recognition accuracy of the system. In future work, we will improve the restoration accuracy and the robustness of the proposed method by combining the face model such as AAM.

References

[1] V. Blanz and T. Vetter. Face recognition based on fitting a 3D morphable model. *IEEE Trans. Pattern Anal. Machine Intell.*, 25(9):1063–1074, 2003. 1

[2] T. Cootes, G. Edward, and C. Taylor. Active appearance models. *IEEE Trans. Pattern Anal. Machine Intell.*, 23(6):681–685, 2001. 1

[3] T. Cootes, C. Taylo, D. Cooper, and J. Graham. Active shape models — their training and application. *Computer Vision and Image Understanding*, 61(1):38–59, 1995. 1

[4] D. Cristinacce and T. Cootes. A comparison of shape constrained facial feature detectors. *Proc. Int'l Conf. Automatic Face and Gesture Recognition*, pages 375–380, 2004. 4

[5] P. Flynn, T. Scruggs, K. Bowyer, C. Jin, K. Hoffman, J. Marques, M. Jaesik, and W. Worek. Overview of the face recognition grand challenge. *Proc. IEEE Computer Society Conf. Computer Vision and Pattern Recognition*, pages 947–954, 2005. 2, 5

[6] R. Gross, I. Matthews, J. Cohn, T. Kanade, and S. Baker. Multi-PIE. *Proc. Int'l Conf. Automatic Face and Gesture Recognition*, pages 1–8, 2008. 2, 5

[7] A. Leonardis and H. Bishof. Robust recognition using eigen images. *Computer Vision and Image Understanding*, 78(1):99–118, 2000. 1, 2

[8] D. Lin and X. Tang. Quality-driven face occlusion detection and recovery. *Proc. IEEE Computer Society Conf. Computer Vision and Pattern Recognition*, pages 1–7, 2007. 1

[9] R. Min, A. Hadid, and J. Dugelay. Improving the recognition of faces occluded by facial accessories. *Proc. of IEEE Int'l Conf. Automatic Face and Gesture Recognition and Workshops*, 26(3):442–447, 2011. 1

[10] P. Phillips, P. Flynn, J. Beveridge, W. Scruggs, A. O'Toole, D. Bolme, K. Bowyer, B. Draper, G. Givens, and Y. Lui. Overview of the multiple biometrics grand challenge. *Lecture Notes in Computer Science (Proc. Int'l Conf. Biometrics)*, 5558:705–714, 2009. 2, 5

[11] P. Phillips, H. Wechsler, J. Huang, and P. Rauss. The FERET database and evaluation procedure for face recognition. *Image and Vision Computing*, 16(5):295–306, 1993. 2, 5

[12] M. Storer, P. Roth, M. Urshiler, and H. Bischof. Fast-robust PCA. *Lecture Notes in Computer Science (Proc. European Conf. Opt. Commun.)*, 5575:130–139, 2009. 1, 2, 3

[13] M. Storer, P. Roth, M. Urshiler, H. Bischof, and J. Birchbauer. Active appearance model fitting under occlusion using fast-robust PCA. *Proc. Int'l Conf. Computer Vision Theory and Applications*, pages 130–137, 2009. 1

[14] M. Storer, M. Urshiler, and H. Bischof. Occlusion detection for ICAO compliant facial photographs. *Proc. IEEE Com-*

Table 2. Experimental results for the gray-scale images.

		PCA	FR-PCA (K)				Proposed (T)			
			256	512	1024	2048	0	1	2	4
Computation time [msec]		2.36	37.49	43.33	55.28	71.39	51.92	54.67	58.01	66.64
RMS error [pixel value] Reconstructed image	w/o occ.	4.33	12.84	11.10	10.13	9.56	11.33	9.56	9.39	9.44
	w/ occ.	25.82	21.74	18.84	16.83	16.06	18.74	13.43	11.27	10.56
RMS error [pixel value] Restored image	w/o occ.	0.00	12.83	11.08	10.06	9.44	2.65	2.34	2.44	2.54
	w/ occ.	17.81	21.74	18.82	16.77	15.93	8.80	6.32	4.92	4.54

Table 3. Experimental results for the color images.

		PCA	FR-PCA (K)				Proposed (T)			
			256	512	1024	2048	0	1	2	4
Computation time [msec]		7.05	100.79	121.95	155.24	206.51	134.57	141.31	155.57	183.82
RMS error [pixel value] Reconstructed image	w/o occ.	5.48	15.42	14.61	14.08	13.64	11.98	10.70	10.58	10.61
	w/ occ.	32.58	14.55	13.69	13.20	12.90	16.66	13.53	12.49	11.86
RMS error [pixel value] Restored image	w/o occ.	0.00	15.14	14.23	13.59	13.03	3.23	2.96	3.00	3.10
	w/ occ.	23.44	14.31	13.36	12.76	12.32	7.23	5.96	5.31	4.99

puter Society Conf. Computer Vision and Pattern Recognition, pages 122–129, 2010. 1

[15] C. Tu and J. Lien. Facial occlusion reconstruction: Recovering both the global structure and the local detailed texture components. *Lecture Notes in Computer Science (Proc. 2nd Pacific-Rim Conf. Advances in Image and Video Technology)*, 4872:141–151, 2007. 1

[16] P. Viola and M. Jones. Rapid oeject detection using a boosted cascade of simple features. *Proc. IEEE Computer Society Conf. Computer Vision and Pattern Recognition*, pages 511–518, 2001. 4